Int. J. Heat Mass Transfer. Vol. 14, pp. 1377–1394. Pergamon Press 1971. Printed in Great Britain

A GENERAL TECHNIQUE FOR THE PREDICTION OF VOID DISTRIBUTIONS IN NON-STEADY TWO-PHASE FORCED CONVECTION

W. T. HANCOX
Canadian Westinghouse Co. Ltd., Atomic Power Division, Hamilton, Ontario, Canada

and

W. B. NICOLL†
Department of Mechanical Engineering, University of Waterloo, Waterloo, Ontario, Canada

(*Received* 15 *September* 1970 *and in revised form* 7 *December* 1970)

Abstract—An analytical technique is presented for the prediction of non-steady void and enthalpy distributions in forced convection flow-boiling water. The analysis is based on the cross section averaged form of the mass and energy conservation equations. Auxiliary relations, based on a local condition hypothesis, have been developed to describe (i) the effect of non-uniform void and velocity profiles and (ii) the vapour generation rate. Predictions of steady flow axial void distributions are shown to be in good agreement with the available data, as are predictions of void oscillation amplitude and phase lag for modulated heat flux data.

NOMENCLATURE

A,	cross section area;
C_0,	$\equiv \langle \alpha v\rangle / \langle \alpha\rangle \langle v\rangle$;
C_1,	$= \langle (1-\alpha) i_l\rangle / \langle 1-\alpha\rangle \langle i_l\rangle$;
C_2,	$= \langle (1-\alpha) v_l i_l\rangle / \langle (1-\alpha) v_l\rangle \langle i_l\rangle$;
c_p,	liquid specific heat;
D_e,	equivalent diameter;
f,	frequency;
h,	heat transfer coefficient;
h^*,	$= c_p \dot{q}''/h_0 \Delta i$;
i,	enthalpy;
i^*,	$= (i_f - i_l)/\Delta i$;
Δi,	evaporation enthalpy $= (i_g - i_f)$;
Δi_i,	inlet subcooling $= i_f - i_{l_i}$;
k,	liquid thermal conductivity;
$\dot{m}$,	mass flux;
P,	pressure;
Pr,	liquid Prandtl no.;
p_h;	heated perimeter;
$\dot{q}''$,	heat flux;
R,	pipe radius;
Re,	Reynolds no. $= \rho_l v_l D_e/\mu$;
T,	temperature;
ΔT,	$= T_s - T$;
t,	time;
v,	velocity;
y^+,	dimensionless distance from the wall $= y/R$;
z,	axial position;
z_1,	$= \dot{m}\Delta i_i/\dot{q}''\ p_h$;
α,	vapour volume fraction;
$\Delta\alpha_{pp}$,	peak-to-peak void amplitude;
Γ,	vapour generation rate;
Γ_m,	$= \dot{q}''\ p_h/A\Delta i$;
ρ,	density;
$\Delta\rho$,	$= \rho_l - \rho_v$;
μ,	liquid viscosity;
ω,	angular frequency;
Φ,	angular phase lag;
ε,	$= (\dot{q}'' - \dot{q}''_0)/\dot{q}''_0$.

Subscripts

b,	bubble layer;

† Presently visiting professor: Centro Tecnologico, Universidade Federalde Santa Catarina, Brazil.

c, center line;
f, saturated liquid;
g, saturated vapour;
h, heated portion of channel;
i, channel inlet;
l, liquid;
o, position of significant vapour formation or steady-state value;
s, saturation condition;
v, vapour;
w, wall.

Superscripts
$*$, dimensionless length w.r.t. z_h;
$^+$, dimensionless length w.r.t. z_l;
$'$, dimensionless length w.r.t. D_e.

1. INTRODUCTION

THE PREDICTION of non-steady phenomena in forced convection flow boiling systems is of considerable importance in nuclear reactor design. The response of the volumetric concentration of the liquid and vapour phases due to perturbations in heat flux and inlet flow is of particular interest due to its influence on the neutron dynamics. The present paper presents an analytical technique for the prediction of the void response to specified perturbations in heat flux and inlet flow.

Various authors have presented void-distribution prediction methods, e.g. the methods reported in [1–6]. In all cases one or more of the following are assumed:

(i) one-dimensional flow
(ii) axially uniform heat flux
(iii) temporally uniform heat flux
(iv) steady inlet velocity
(v) linearized conservation equations, and
(vi) thermal equilibrium between the vapour and liquid phases.

The present method includes none of the above restrictions.

The analysis most closely related to the present work is that presented by Zuber and Staub [3]. They have presented a comprehensive analysis of the void response to both heat flux and inlet flow modulation assuming negligible inertial effects, thermal equilibrium between the phases, and incompressible phases. Further, they assumed that the effects of non-uniform void and velocity profiles did not vary axially. Under these assumptions the void response is completely defined by a void propagation equation for which closed form solutions exist. The present authors have extended this analysis to consider flows having non-zero inlet subcooling, i.e. flows for which the assumptions of thermal equilibrium and fully developed void, velocity and enthalpy profiles are not valid. In this analysis the mass and energy conservation equations are phrased in the form of a void and an enthalpy propagation equation which incorporate a function describing the local vapour generation rate and distribution parameters to represent the effects of radial distributions of void, velocity and enthalpy. The vapour generation has been developed employing a simple physical model similar to that presented by Larsen and Tong [4]. At present both a physical model and systematic experimental data to determine the complete dependence of the distribution parameters on local conditions are not available. In this analysis the void-velocity distribution parameter relation developed in [6] has been adopted, except where otherwise noted, and all other distribution effects have been neglected. Both the vapour generation function and the void-velocity distribution parameter are assumed to depend only on local instantaneous properties. An implicit finite difference scheme has been employed to solve the governing equations.

The accuracy of the numerical solution is demonstrated by comparison with a closed form solution. Comparisons of predictions with the steady-state axial void distributions presented in [2, 7–11] and the transient void distributions presented by St. Pierre [2] for heat flux modulation show good agreement.

2. DERIVATION OF THE GOVERNING EQUATIONS

2.1 *The void and enthalpy propagation equations*

For a differential length of channel the cross section averaged mass and energy conservation equations are as follows. The continuity requirement for the vapour phase may be written as

$$\frac{\partial}{\partial t}\langle\alpha\rho_v\rangle + \frac{\partial}{\partial z}\langle\alpha\rho_v v_v\rangle = \langle\Gamma\rangle \qquad (1)$$

where $\langle\Gamma\rangle$ = vapour generation rate

$\langle\ \rangle$ denotes the operator $\frac{1}{A}\int_A (\ )\,\mathrm{d}A$.

Similarly, the liquid phase continuity equation is

$$\frac{\partial}{\partial t}\langle(1-\alpha)\rho_l\rangle + \frac{\partial}{\partial z}\langle(1-\alpha)\rho_l v_l\rangle = -\langle\Gamma\rangle. \qquad (2)$$

At present there are insufficient experimental data to support a detailed description of the interphase energy transfer mechanisms. The need for this detailed description is avoided through the use of the mixture energy equation which has the following form

$$\frac{\partial}{\partial t}\langle\alpha\rho_v i_v + (1-\alpha)\rho_l i_l\rangle + \frac{\partial}{\partial z}\langle\alpha\rho_v v_v i_v + (1-\alpha)\rho_l v_l i_l\rangle = \frac{q'' p_h}{A}. \qquad (3)$$

The interphase energy transfer will be introduced later in the form of a semi-empirical vapour generation equation, based on a highly simplified physical model.

In the following derivations we will make use of the simplifications listed below:

(i) the vapour and liquid saturation properties will be assumed spatially and temporally invariant.

(ii) zero local drift between the phases will be assumed; i.e. at a point the liquid and vapour velocities will be assumed equal although the average cross section velocities may not be.

It is appropriate to note that these simplifying assumptions, while not necessary, yield a tractable system of equations and appear reasonable for most applications of interest. The former assumption may be replaced with equations of state and the momentum conservation equation. A relation describing the local relative velocity between the phases is required to remove the latter assumption.

First consider the continuity equations. Addition of (1) and (2) gives

$$\frac{\partial}{\partial z}\langle v\rangle = \frac{\Delta\rho\langle\Gamma\rangle}{\rho_l\rho_v}. \qquad (4)$$

Equation (4) can be integrated to obtain the following expression for the axial velocity distribution

$$\langle v\rangle = v_i(t) + \int_0^z \frac{\Delta\rho\langle\Gamma\rangle}{\rho_l\rho_v}\,\mathrm{d}z. \qquad (5)$$

The vapour continuity equation, equation (1), may be expanded to obtain

$$\frac{\partial\langle\alpha\rangle}{\partial t} + C_0\langle v\rangle\frac{\partial\langle\alpha\rangle}{\partial z} + C_0\langle\alpha\rangle\frac{\partial\langle v\rangle}{\partial z} + \langle\alpha\rangle\langle v\rangle\frac{\partial C_0}{\partial z} = \frac{\langle\Gamma\rangle}{\rho v}$$

where

$$C_0 \equiv \langle\alpha v\rangle/\langle\alpha\rangle\langle v\rangle.$$

Employing equation (4) and rearranging the above equation becomes

$$\frac{\partial\langle\alpha\rangle}{\partial t} + C_0\langle v\rangle\frac{\partial\langle\alpha\rangle}{\partial z} + \langle\alpha\rangle\langle v\rangle\frac{\partial C_0}{\partial z} = \left[1 - C_0\langle\alpha\rangle\frac{\Delta\rho}{\rho_l}\right]\frac{\langle\Gamma\rangle}{\rho_v}. \qquad (6)$$

An examination of steady flow data [6] indicates that the distribution parameter, C_0, can be considered, for a given geometry and at moderate to large mass velocities to be a function of the average void $\langle\alpha\rangle$;

$$\frac{\partial C_0}{\partial z} = \frac{\partial C_0}{\partial\langle\alpha\rangle}\frac{\partial\langle\alpha\rangle}{\partial z}.$$

Upon substitution of this result, equation (6) may be written in the form

$$\frac{\partial\langle\alpha\rangle}{\partial t} + V_\alpha\frac{\partial\langle\alpha\rangle}{\partial z} = \Omega_\alpha \qquad (7)$$

where

$$V_\alpha = \left[C_0 + \frac{\partial C_0}{\partial\langle\alpha\rangle}\langle\alpha\rangle\right]\langle v\rangle$$

$$\Omega_\alpha = \left[1 - C_0\langle\alpha\rangle\frac{\Delta\rho}{\rho_l}\right]\frac{\langle\Gamma\rangle}{\rho_v}.$$

Equation (7), we observe, has the form of a propagation equation. Zuber and Staub [3], as noted above, have presented solutions for a thermal equilibrium flow and C_0 = constant; conditions for which (7) is linear (see Appendix I). For the special case of an adiabatic flow ($\Omega_\alpha = 0$) and C_0 = constant, equation (7) reduces to a homogeneous linear equation which states that void disturbances are propagated at the velocity V_α without change in shape.

Next consider the energy equation for the mixture. In the following we will assume that the vapour is at saturation. Experiments [12, 13] indicate that this assumption is valid in the subcooled region, however, it is appropriate to observe that it will become less valid, due to vapour super-heating, as the void approaches unity, although it appears that solutions are not appreciably influenced. With this assumption and substitution of equation (1), we can write equation (3) in the form

$$\frac{\partial}{\partial t}\langle(1-\alpha)\rho_l i_l\rangle + \frac{\partial}{\partial z}\langle(1-\alpha)\rho_l v_l i_l\rangle = \frac{q'' p_h}{A} - i_v\langle\Gamma\rangle. \quad (8)$$

It is convenient to introduce the following distribution parameters

$$C_1 \equiv \frac{\langle(1-\alpha)i_l\rangle}{\langle 1-\alpha\rangle\langle i_l\rangle} \quad (9)$$

$$C_2 = \frac{\langle(1-\alpha)v_l i_l\rangle}{\langle(1-\alpha)v_l\rangle\langle i_l\rangle}.$$

Upon substitution of these parameters, equation (8) can be rearranged to obtain

$$C_1\langle 1-\alpha\rangle\frac{\partial\langle i_l\rangle}{\partial t} + C_2(1 - C_0\langle\alpha\rangle)\langle v\rangle\frac{\partial\langle i_l\rangle}{\partial z} - C_1\langle i_l\rangle\frac{\partial\langle\alpha\rangle}{\partial z} - C_2C_0\langle v\rangle\frac{\partial\langle\alpha\rangle}{\partial z} + C_2(1 - C_0\langle\alpha\rangle)\frac{\partial\langle v\rangle}{\partial z} = \frac{q''Ph}{\rho_l A} - i_v\frac{\langle\Gamma\rangle}{\rho_l}.$$

Employing equations (2) and (4) with the assumption $C_2 = C_2(\langle\alpha\rangle)$, the above equation can be rewritten as

$$\frac{\partial}{\partial t}\langle i_l\rangle + V_i\frac{\partial}{\partial z}\langle i_l\rangle = \Omega_i \quad (10)$$

where

$$V_i = \frac{C_2(1 - C_0\langle\alpha\rangle)\langle v\rangle}{C_1(1 - \langle\alpha\rangle)}$$

$$\Omega_i = \frac{(q'' p_h/A) - (i_v - \langle i_l\rangle)\langle\Gamma\rangle}{C_1\rho_l\langle 1-\alpha\rangle} + \left[\left(\frac{C_2}{C_1} - 1\right)(1 - C_0\langle\alpha\rangle)\frac{\Delta\rho}{\rho_v} + \frac{1 - C_1}{C_1}\right]\frac{\langle i_l\rangle\langle\Gamma\rangle}{\rho_l\langle 1-\alpha\rangle} + \left[\frac{V_i}{C_2}\frac{\partial C_2}{\partial\langle\alpha\rangle} + \left(\frac{C_2}{C_1} - 1\right)\frac{V_\alpha}{\langle 1-\alpha\rangle}\right]\frac{\langle i_l\rangle}{\rho_l}\frac{\partial\langle\alpha\rangle}{\partial z}.$$

It is also convenient to introduce the following dimensionless enthalpy

$$i^* = \frac{i_f - \langle i_l\rangle}{\Delta i}.$$

Equation (10) becomes

$$\frac{\partial i^*}{\partial t} + V_i\frac{\partial i^*}{\partial z} = \Omega_i^* \quad (11)$$

where

$$\Omega_i^* = -\frac{\Gamma_m - (1 + i^*)\langle\Gamma\rangle}{C_1\rho_1\langle 1-\alpha\rangle} + \left[\left(\frac{C_2}{C_1} - 1\right)(1 - C_0\langle\alpha\rangle)\frac{\Delta\rho}{\rho_v} + \frac{1 - C_1}{C_1}\right]\frac{\langle i_l\rangle\langle\Gamma\rangle}{\rho_l\Delta i\langle 1-\alpha\rangle} + \left[\frac{V_i}{C_2}\frac{\partial C_2}{\partial\langle\alpha\rangle} + \left(\frac{C_2}{C_1} - 1\right)\frac{V\alpha}{\langle 1-\alpha\rangle}\right]\frac{\langle i_l\rangle}{\rho_l\Delta i}\frac{\partial\langle\alpha\rangle}{\partial z}.$$

For C_1 and C_2 equal to unity, approximated at low subcooling where the radial distribution of

$\langle i_l \rangle$ is nearly uniform, equation (11) becomes

$$\frac{\partial i^*}{\partial t} + \frac{(1 - C_0\langle \alpha \rangle)\langle v \rangle}{\langle 1 - \alpha \rangle} \frac{\partial i^*}{\partial z} = - \frac{\Gamma_m - (1 + i^*)\langle \Gamma \rangle}{\rho_l \langle 1 - \alpha \rangle}. \quad (12)$$

2.2 *Vapour generation function*

To determine the appropriate form for the vapour generation function, consider steady-state flow in a circular tube as presented in Fig. 1. The single-phase region will extend to the point z_s, at which the wall temperature first reaches saturation, beyond z_s bubbles may form at the wall. The presence of bubbles increases the effective conductivity in the near wall region and hence reduces the resistance to heat transfer through the bubble layer to the liquid core. In this region of attached void the heat flux that could be transferred to the liquid core, $\dot{q}_b''$, based on the effective conductivity and mean liquid subcooling with the "edge" of the bubble layer at the saturation temperature, is greater than the specified wall heat flux, hence vapour formation is suppressed. As the fluid progresses downstream the liquid subcooling is further reduced resulting in a reduced potential heat flux $\dot{q}_b''$. When the effective thermal conductivity at the outer edge of the bubble layer is no longer sufficient, given the existing temperature gradient, to remove the specified heat flux, $\dot{q}_w''$ vapour generation must begin. This point will be denoted by z_0. Thus upstream of z_0 the vapour generation is effectively zero. At the other extreme, as the liquid enthalpy approaches saturation a thermal equilibrium state is approached and the vapour generation rate is a simple function of the local heat flux and evaporation enthalpy defined explicitly by the energy equation.

Based on the postulated physical events

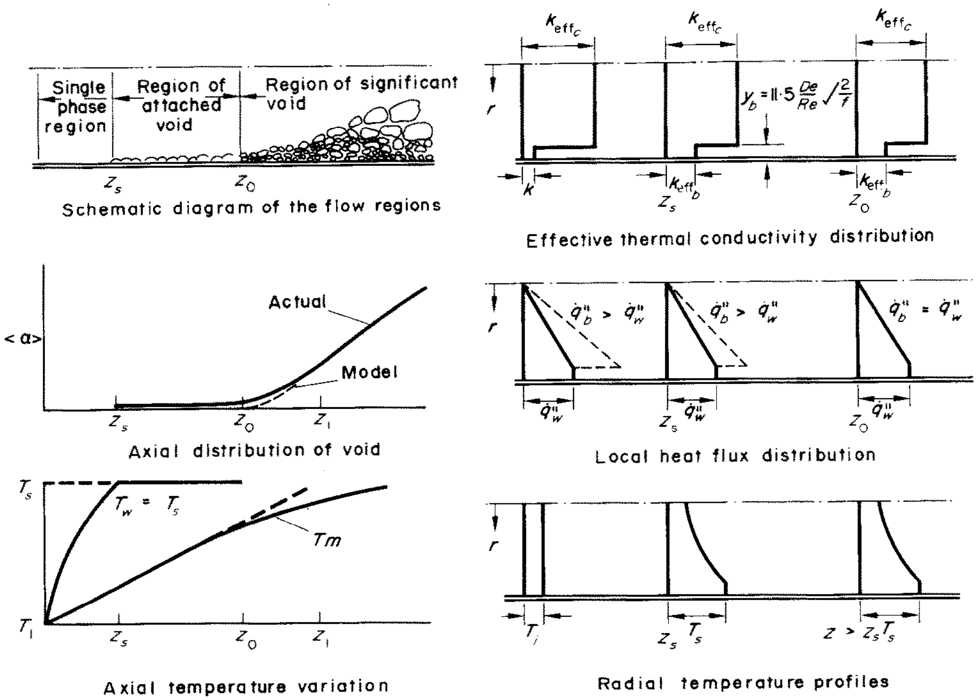

FIG. 1. A simplified model for the subcooled region.

upstream of z_0, an analysis [6], employing logarithmic velocity and temperature profiles and a turbulent Prandtl number of unity in the liquid core, yields the following relationship defining the position of significant vapour formation

$$z_0^+ = 1 - \frac{F}{z_1'}. \qquad (13)$$

The function F has been determined by examining the available experimental data [2, 7–11] the following form has been found to adequately represent the data

$$F = 0{\cdot}624\,(Re)^{0{\cdot}338}.$$

We note that, since z_0^+ can be expressed as

$$z_0^+ = 1 - \frac{\Delta T_0}{\Delta T_i}$$

the following heat transfer coefficient is implied

$$h_0 = 0{\cdot}40\frac{k}{D_e}(Re)^{0{\cdot}662}\,Pr. \qquad (14)$$

For the region downstream of z_0 consider the separated flow model shown in Fig. 2. Assuming

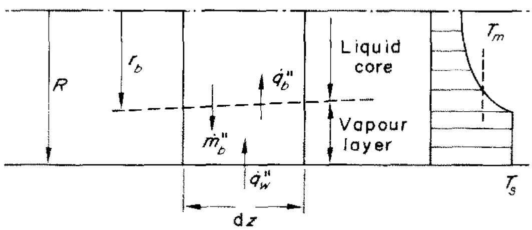

FIG. 2. Separated phase model employed to determine the form for the vapour generation function.

that the vapour–liquid interface is at the saturation temperature the conservation equations for an infinitesimal control volume enclosing the vapour layer are;
(i) continuity

$$\frac{\mathrm{d}}{\mathrm{d}z}\int_{r_b}^{R} \rho_g v 2\pi r \mathrm{d}r = 2\pi r_b \dot{m}_b'' \qquad (15)$$

where $\dot{m}_b''$ = liquid mass flux across the phase interface
(ii) energy

$$\frac{\mathrm{d}}{\mathrm{d}z}\int_{r_b}^{R} \rho_g i_g v 2\pi r \mathrm{d}r - 2\pi r_b \dot{m}_b'' i_f = 2\pi(R\dot{q}_w'' - r_b\dot{q}_b''). \qquad (16)$$

Substituting equation (15) into (16) we obtain the following expression for the mass rate of vapour generation per unit area of the interface

$$\dot{m}_b'' = \frac{\dot{q}_w'' - (r_b/R)\,\dot{q}_b''}{(r_b/R)\,\Delta i}.$$

The above expression may be rewritten in terms of cross-section averaged variables as

$$\langle\Gamma\rangle = \frac{4\dot{q}_w''}{D_e\Delta i}\left[1 - (1-\alpha)^{\frac{1}{2}}\frac{\dot{q}_b''}{\dot{q}_w''}\right]. \qquad (17)$$

The heat transfer to the liquid core $\dot{q}_b''$ is assumed proportional to the local liquid subcooling, such that

$$\dot{q}_b'' = \frac{h}{c_p}(i_f - i_l) \qquad (18)$$

where h is an appropriate heat transfer coefficient. For the present we will assume that $h = h_0$ everywhere in the boiling region; this assumption has been successfully employed by Ahmad [5]. We note that this assumption is also probably invalid as the void approaches unity. It does not, however, influence the calculations since i_l approaches i_f as the void approaches unity. Employing equations (14), (17) and (18) and the observations presented above for $z < z_0$, the vapour generation rate will be represented by the following piece-wise continuous function

$$\begin{aligned} \langle\Gamma\rangle &= \Gamma_m[1 - (1-\alpha)^{\frac{1}{2}} i^*/h^*] \qquad & i^* \leq h^* \\ \langle\Gamma\rangle &= 0 & i^* > h^* \end{aligned} \qquad (19)$$

where

$$h^* = c_p\dot{q}_w''/h_0\Delta i$$

$$\Gamma_m = 4\dot{q}_w''/D_e\Delta i.$$

Equation (19) displays the appropriate asymptotic behaviour, since $\langle \Gamma \rangle$ approaches the thermal equilibrium generation rate Γ_m, as the liquid subcooling i^* approaches zero. We note that the $(1 - \alpha)^{\frac{1}{2}}$ multiplier results from the assumption that vapour–liquid interface area is proportional to $(1 - \alpha)$. While this is an approximation it does lead, when combined with the assumption of a constant heat transfer coefficient, to an exponential variation of mean liquid temperature such as has been observed by Staub [12].

2.3 *Distribution parameters*

As noted above, a consequence of employing the cross section averaged form of the conservation equation is that it is necessary to introduce distribution parameters to represent the effects of nonuniform radial void, velocity and enthalpy profiles. The following distribution parameters have been introduced above

$$C_0 \equiv \langle \alpha v \rangle / \langle \alpha \rangle \langle v \rangle$$

$$C_1 = \langle (1 - \alpha) i_l \rangle / \langle 1 - \alpha \rangle \langle i_l \rangle$$

$$C_2 = \langle (1 - \alpha) v_l i_l \rangle / \langle (1 - \alpha) v_l \rangle \langle i_l \rangle .$$

At present we lack both a physical model and systematic experimental data from which the complete dependence of C_0, C_1 and C_2 on the parameters of interest could be determined. There is, however, some experimental evidence [12, 13] to suggest that the liquid enthalpy profiles may be assumed uniform, within the present range of interest, and hence we will set $C_1 = C_2 = 1$. It is pertinent to note that this assumption has been successfully employed in steady flow analyses [6, 14]. The influence of the parameter C_0 has been studied in some detail by Zuber *et al.* [14, 15] and the present authors [6]. It is to the evaluation of an empirical relation for C_0 that we now turn.

To evaluate C_0 we require radial distributions of void and velocity. Unfortunately simultaneous measurements of developing void and velocity distributions are not available. However, radial void distributions for steady flow have been presented by St. Pierre [2]. These can be used in conjunction with realistic hypothetical velocity profiles to obtain the axial variation of C_0. Figure 3 shows the axial variation of C_0

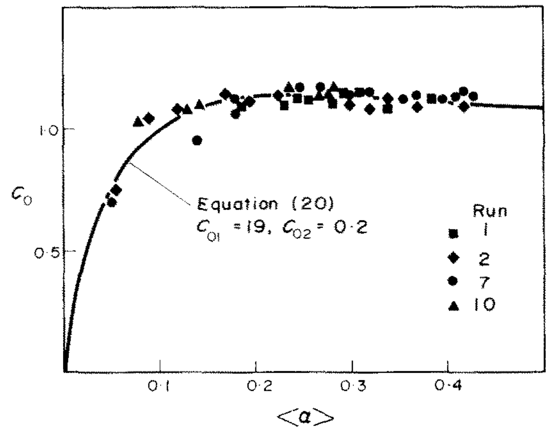

FIG. 3. Axial variation of C_0 for St. Pierre's data [2].

evaluated assuming power-law profiles of the form:

$$\frac{\alpha - \alpha_C}{\alpha_w - \alpha_C} = (y^+)^n$$

$$\frac{v - v_C}{v_C} = -(y^+)^m .$$

Values of n have been obtained by a least squares fit of the void power-law profile to the data, and the power m such that

$$m = 7 \text{ for } \alpha_w > 0$$

$$m = n \text{ for } \alpha_w = 0 .$$

Arguments justifying the use of similar void and velocity profiles have been presented by Zuber *et al.* [14]. The resulting axial variations of C_0 are consistent with what we would expect. It is easy to argue, from the definition, that C_0 must have a near zero value at the start of the significant void region, since in this region the void is concentrated in the low-velocity near-wall region. At the other extreme C_0 must approach unity as the average void approaches unity. Values of $C_0 > 1$ at intermediate values of $\langle\alpha\rangle$ are consistent with Bankoff's [16] observation that bubbles tend to concentrate in the high-velocity tube-center region after some development length.

In the present work we have adopted the following function which embodies the above behaviour

$$C_0 = \frac{1 - \exp(-C_{01}\alpha)}{1 - \exp(-C_{01})}(1 + C_{02}) - C_{02}\alpha \quad (20)$$

where C_{01} and C_{02} are constants determined to obtain the best fit to the experimental data. The values obtained for St. Pierre's data are

$$C_{01} = 19$$
$$C_{02} = 0{\cdot}2.$$

It is appropriate to observe here that some disagreement exists between the values of C_{02} obtained from the data of various investigators. In another more extensive study [6] the present authors found that the best overall predictions for the steady-state void-distribution data of six investigators [2, 7–11] were obtained with

$$C_{02} = 1{\cdot}164 - 1{\cdot}14 \times 10^{-3}P + 0{\cdot}357 \times 10^{-6}P^2. \quad (21)$$

It appears that these differences may be due to geometrical peculiarities of the individual apparatuses, and thus we have set $C_{02} = 0{\cdot}2$ when comparing predictions with St. Pierre's data and equation (21) has been employed in all other cases. The consequences of this procedure will be examined in greater detail below.

2.4 *Method of solution*

Axial void and enthalpy distributions can be obtained by the simultaneous solution of equations (7) and (8), the void and enthalpy propagation equations, subject to the following boundary and initial conditions:

(i) heat flux, $\dot{q}'' = \dot{q}''(t, z)$
(ii) inlet velocity, $v_i = v_i(t)$
(iii) inlet subcooling, $\Delta T_i = \Delta T_i(t)$.

In the present analysis the auxiliary relations defining the distribution parameter, C_0, and the vapour generation rate, $\langle\Gamma\rangle$, are functions of the local void and enthalpy. Hence the void and enthalpy propagation equations are non-linear and an implicit finite difference solution has been employed; this solution form is described in detail in Appendix II. The implicit finite difference scheme can be shown to be inherently stable for more simple forms of the propagation equation [17] and hence is appropriate for the present application.

The accuracy of the numerical technique is demonstrated by comparison with a closed form solution of the void propagation equation presented by Zuber and Staub [3]; the peak-to-peak void amplitude and phase lag for heat flux modulation are presented in Appendix I. Comparisons of the void wave form and the peak-to-peak void amplitude are shown in Fig. 4. For

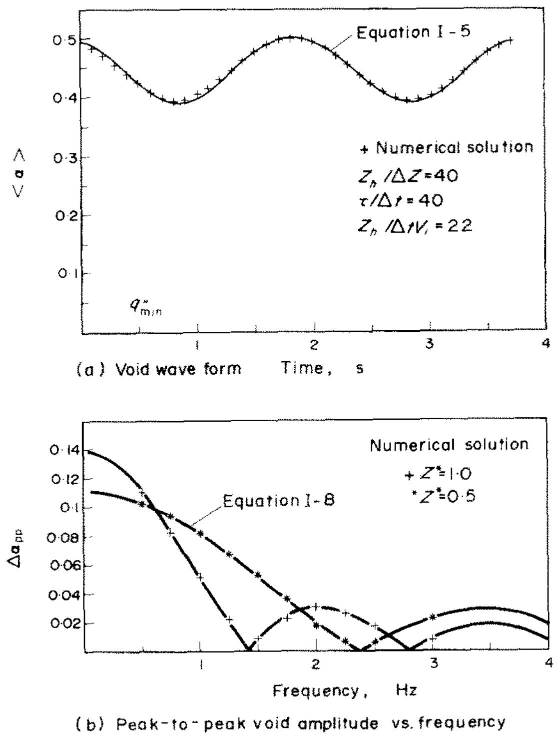

FIG. 4. Comparison of the numerical solution with a closed form solution.

this particular application excellent agreement between the numerical and closed form solutions was obtained for space and time step sizes selected such that,

$$\Delta z < z_h/20$$
$$\Delta t < \tau/20$$

where τ = minimum of $1/f$ or z_h/v_i.

3. COMPARISON OF PREDICTION WITH EXPERIMENT

Two classes of experimental results will be examined: axial void distributions for steady flow and axially uniform heat flux; and axial void distributions for steady flow with modulated heat flux. The former class was chosen in spite of its restricted nature because of the large amount of available experimental data covering a wide range of flow, pressure, heat flux, and subcooling. Comparison of experiment with prediction will allow the evaluation of the accuracy and generality of the vapour generation function and the distribution parameters. The modulated heat flux data were chosen to test the prediction scheme for non-steady conditions.

3.1 *Axial void distributions for steady flow and uniform heat flux*

Predicted void distributions have been compared with 96 experimental distributions given in [2, 7–11]. Table 1 summarizes the range of geometric and experimental conditions included. Typical comparisons are shown in Figs. 5–10.

It may be seen that the predictions are generally good. There is no systematic variation of error with any of the experimental conditions. This satisfactory result implies that the vapour generation function and the distribution parameters employed are adequate over the wide range of conditions examined.

The overall root-mean-square error for all 96 comparisons was 5 per cent, an amount probably nearly equal to the experimental scatter and an amount equal to or less than the root-mean-square error obtained with available steady flow uniform heat flux void prediction techniques [18].

Table 1. Range of steady-state data examined

Author	No. of data points	Heat flux, Btu/sft^2	pressure psia	Inlet velocity, ft/s	Inlet subcooling, °F	Rectangular test sections		
						Flow area, in.^{2}	Heated perimeter, in.	Length
Maurer	12	27 ↓ 170	1200 ↓ 2000	2 ↓ 6	50 ↓ 300	0·088	1·88	27
Marchaterre	30	5 ↓ 25	163 ↓ 615	1 ↓ 6	3 ↓ 20	0·5	4·5	60
Foglia	35	30 ↓ 120	700 ↓ 1300	9 ↓ 18	12 ↓ 112	0·050	2·1	27
Egen	14	11 ↓ 110	2000	3·5 ↓ 6	6 ↓ 194	0·103	2·21	27
St. Pierre	10	6 ↓ 25	200 ↓ 800	2·5 ↓ 4·0	0·5 ↓ 13	0·76	4·37	50
Christensen	6	18 ↓ 44	400 ↓ 1000	2·5 ↓ 4·0	6 ↓ 23	0·76	4·37	50

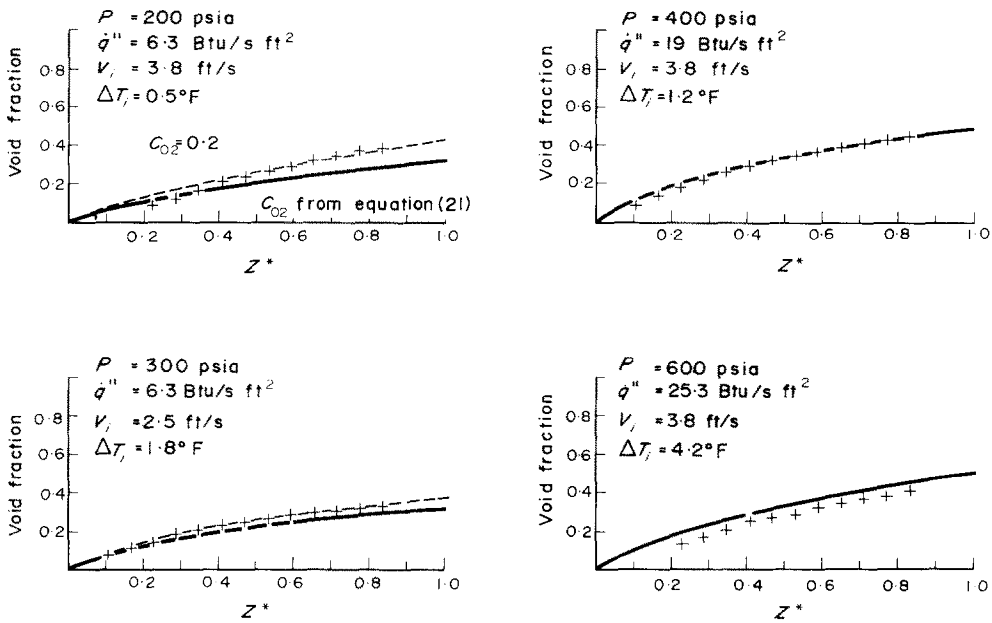

FIG. 5. Predictions for St. Pierre's data [2].

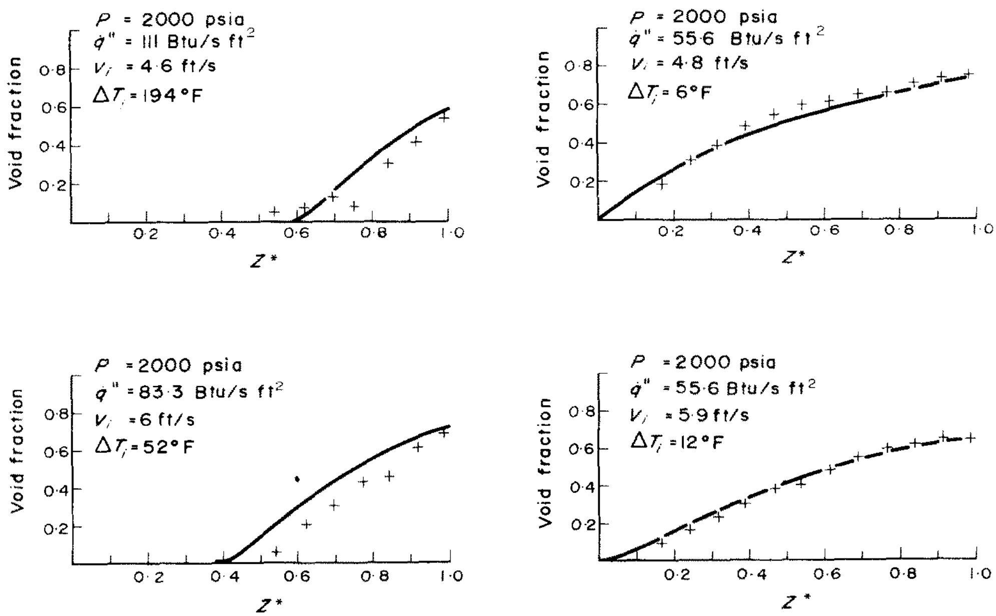

FIG. 6. Predictions for the data of Egen *et al.* [8].

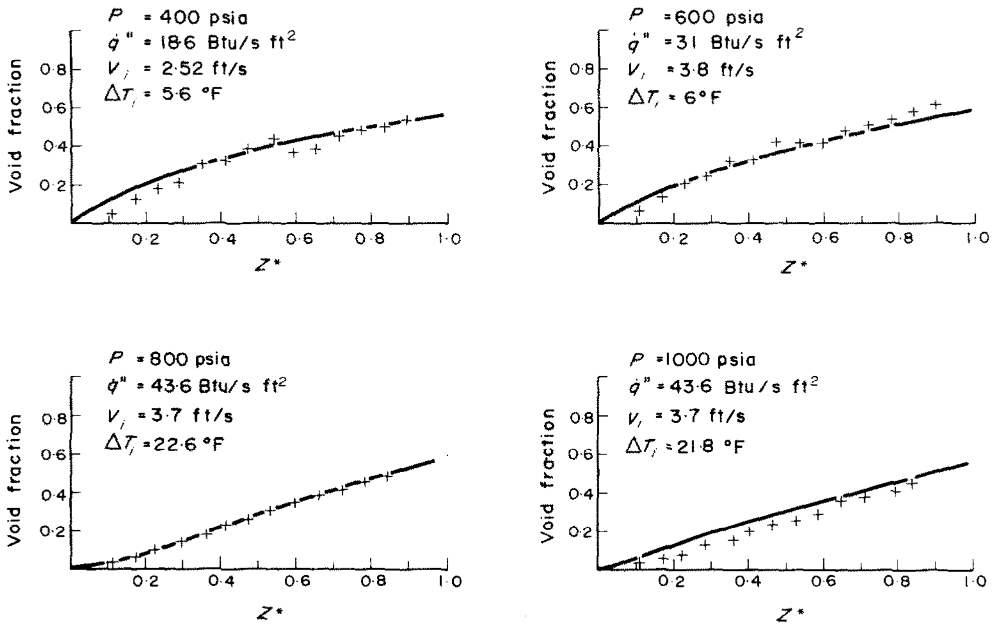

FIG. 7. Predictions for Christensen's data [11].

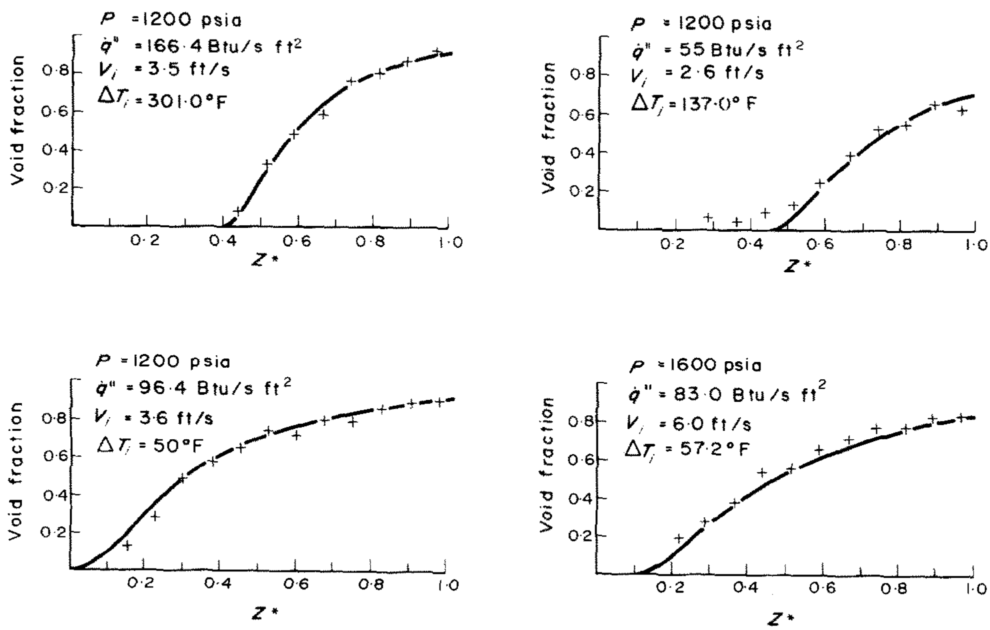

FIG. 8. Predictions for Maurer's data [7].

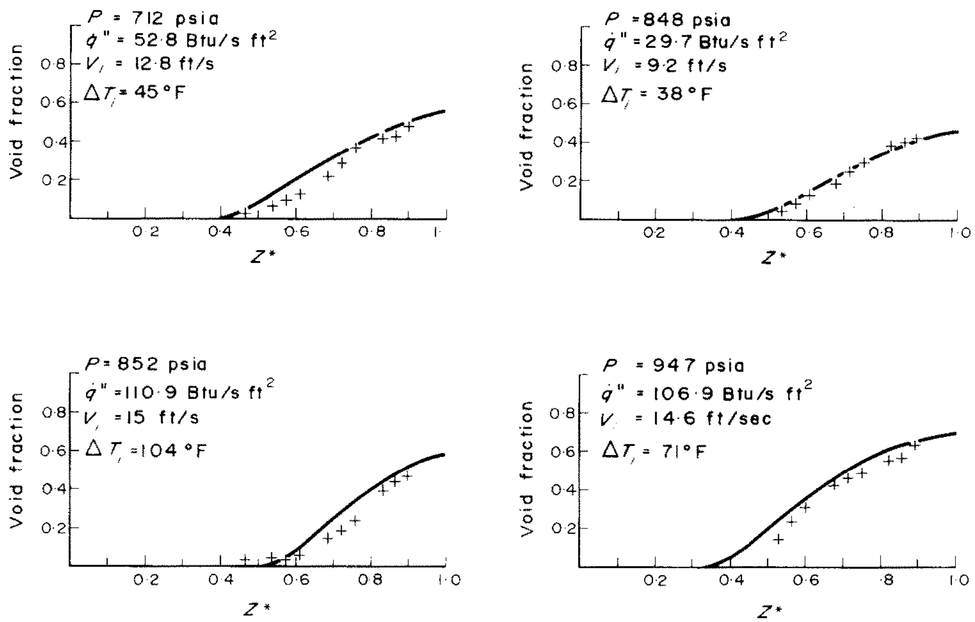

FIG. 9. Predictions for the data of Foglia *et al.* [9].

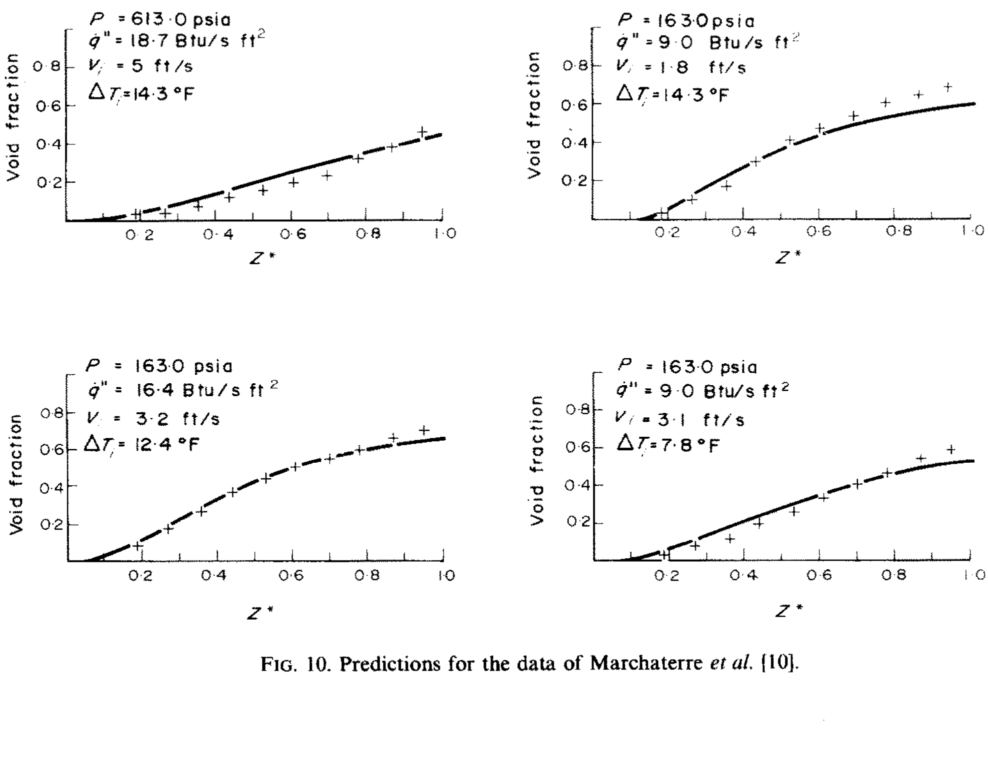

FIG. 10. Predictions for the data of Marchaterre *et al.* [10].

As noted in section 2.3 above, there exists an apparent discrepancy between the "best overall" value of C_{02} and that obtained from St. Pierre's data [2]. The consequence of this discrepancy for steady flow and uniform heat flux can be seen in Fig. 5. We observe that the low pressure predictions are somewhat improved if the modified value of C_{02} is used; at higher pressures the change is negligible. We may conclude that the steady state axial void distribution prediction is relatively insensitive to this modification although, as demonstrated in the next section, this insensitivity is not likely to extend to non-steady conditions.

3.2 *Axial void distributions with heat flux modulation*

Predicted peak-to-peak void amplitudes and phase lags at specified axial positions, for a 10 per cent peak-to-peak sinusoidal heat flux variation, are shown in Figs. 11–16. The data are those obtained by St. Pierre [2].

Again it may be observed that agreement between prediction and experiment is satisfactory; the dependence of both the void amplitude oscillation and the phase lag on the frequency of the heat flux modulation appear to be adequately represented, particularly at the lower frequencies. At higher frequencies the agreement is less satisfactory. It is in this region, however, that the void oscillation amplitudes are small and hence the experimental uncertainties in both amplitude and phase-lag are large.

It is of interest to examine the effects of the inclusion of the non-linear terms in the conservation equations by comparing the present results with the analytical results presented in Section 2.4. The effects are two: first, the minima in the amplitude–frequency plane no longer have the value zero; secondly the phase lag–frequency relation is no longer linear and the frequencies at which the lag equals integral multiples of π do not correspond to the frequencies at which the amplitude–frequency relation displays minima.

The effect of the use of the modified value of

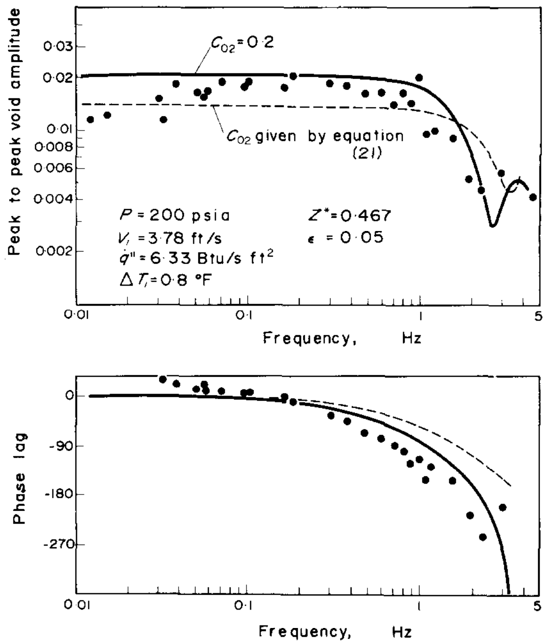

FIG. 11. Predictions for St. Pierre's transient data; run 1, $z^* = 0{\cdot}467$.

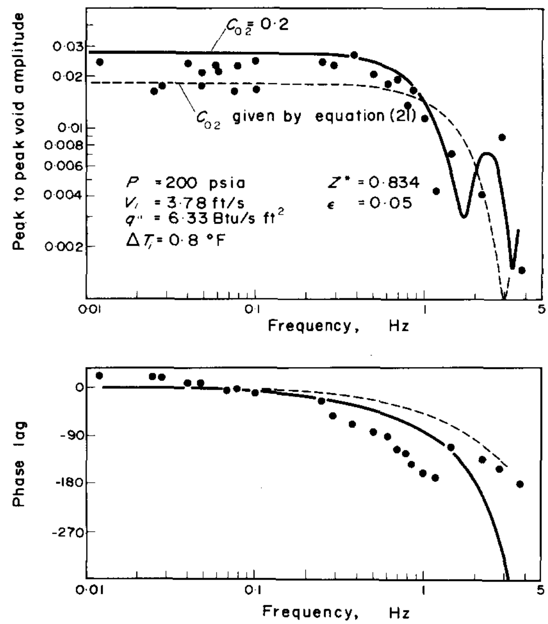

FIG. 12. Predictions for St. Pierre's transient data; run 1, $z^* = 0{\cdot}834$.

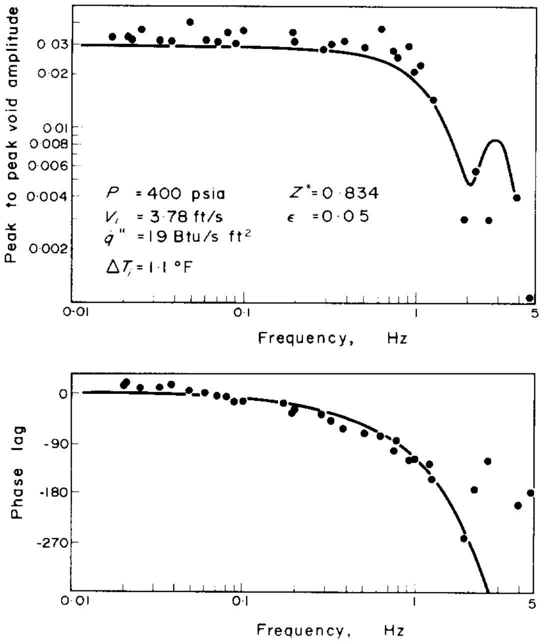

FIG. 13. Predictions for St. Pierre's transient data; run 7, $z^* = 0{\cdot}834$.

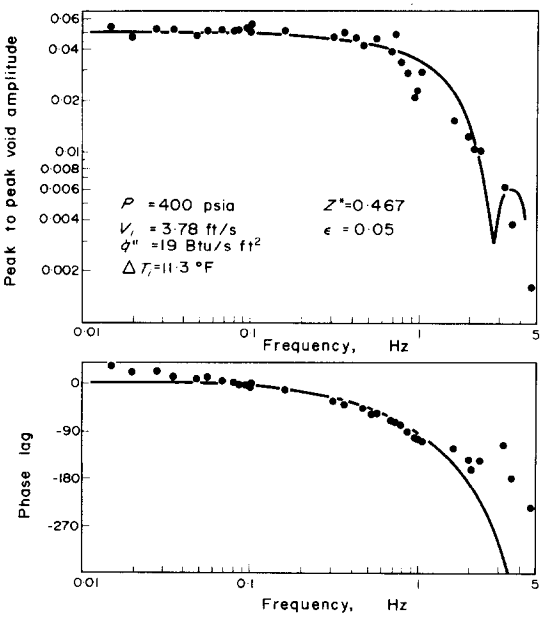

FIG. 14. Predictions for St. Pierre's transient data; run 8, $z^* = 0{\cdot}467$.

C_{02} is also shown in Figs. 11 and 12. It appears that the location of the amplitude minima, the amplitude values, and the phase lag variation are significantly affected by this modification at low pressures. At higher pressures the C_{02} values obtained from the general expression [equation (21)] are comparable to the modified value; hence at higher pressures the results may be expected to be less sensitive to this modification. We conclude that caution should be exercised when attempting to predict non-steady void distributions in other geometries for which the distribution parameters may be expected to be different. Further, the present results indicate that the examination of non-steady void data may be a useful, if indirect method for the determination of the distribution parameter C_0.

4. SUMMARY

An analytical technique has been presented for the prediction of non-steady void and enthalpy distributions in forced convection flow-boiling water. The analysis is based on the cross-section averaged form of the mass and energy conservation equations. Auxiliary relations have been developed to describe (i) the effect of non-uniform void and velocity profiles and (ii) the vapour generation rate. At present these relations depend only on local instantaneous properties. An implicit finite difference scheme has been employed to solve the governing equations.

The accuracy of the numerical solution technique has been demonstrated by comparison with a closed form solution. Predictions of axial void distributions for steady flow and axially uniform heat flux demonstrate the adequacy of the auxiliary relations. An overall root-mean-square error for 96 axial distributions of 5 per cent has been obtained; an amount probably equal to the experimental scatter and equal to or less than the root-mean-square error obtained with available steady flow prediction techniques [18]. Predicted peak-to-peak void amplitudes and phase lags, for a sinusoidal heat flux variation, are shown to agree satisfactorily with

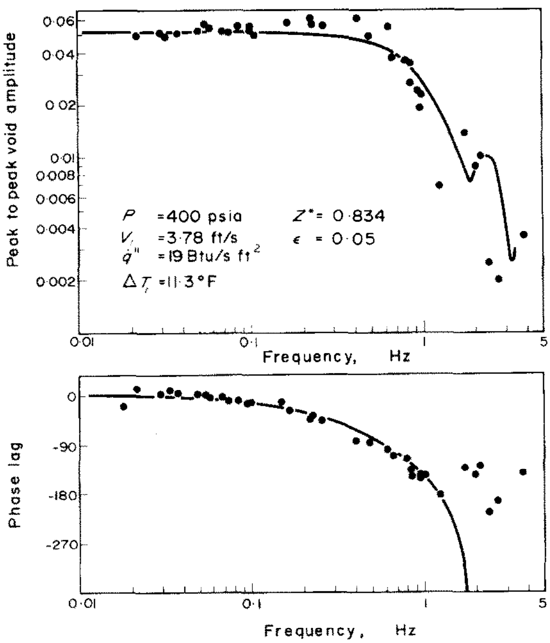

FIG. 15. Predictions for St. Pierre's transient data; run 8, $z^* = 0{\cdot}834$.

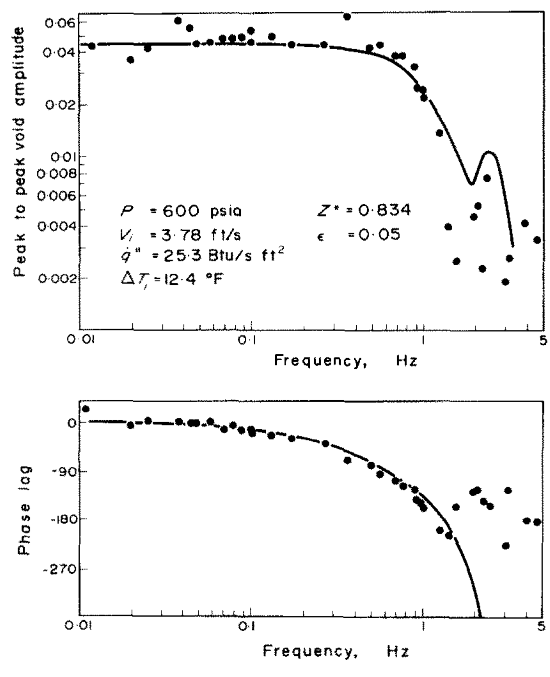

FIG. 16. Predictions for St. Pierre's transient data; run 10, $z^* = 0{\cdot}834$.

St. Pierre's data [2]. A strong dependence of the non-steady void predictions on the void-velocity distribution parameter is indicated.

The available non-steady data do not provide a stringent test of the local conditions hypothesis employed in the development of the auxiliary relations. Further model developments require more extensive non-steady data.

ACKNOWLEDGEMENT

The authors wish to express their thanks to the Advanced Engineering Branch of Atomic Energy of Canada Limited, for permission to publish the analytical work described in this paper.

REFERENCES

1. I. L. HUDSON, K. M. ATIT and S. G. BANKOFF, Response of a boiling channel to power of inlet flow modulation, *Chem. Engng Sci.* **19**, 387–402 (1964).
2. C. C. ST. PIERRE, Frequency-response analysis of steam voids to sinusoidal power modulation in a thin-walled boiling water coolant channel, ANL-7041 (May 1965).
3. N. ZUBER and F. STAUB, The propagation and the wave form of the vapour volumetric concentration in boiling, forced convection system under oscillatory conditions, *Int. J. Heat Mass Transfer* **9**, 871–895 (1966).
4. P. S. LARSEN and L. S. TONG, Void fractions in subcooled flow boiling, *J. Heat Transfer* **91**, 471–476 (1969).
5. S. Y. AHMAD, Axial distribution of bulk temperature and void fraction in a heated channel with inlet subcooling, Unpublished A.E.C.L. report (1969).
6. W. T. HANCOX and W. B. NICOLL, Forced convection boiling; prediction of axial void distributions. Submitted for publication in the *Can. J. Chem. Engng* (1970).
7. G. W. MAURER, A method of predicting steady-state boiling vapour fractions in reactor coolant channels, WAPD-BT-19 (1956).
8. R. A. EGEN *et al.*, Vapour formation and behaviour in boiling heat transfer, Battelle Memorial Institute Report BMI-1163 (February 1957).
9. J. J. FOGLIA *et al.*, Boiling-water void distribution and slip ratio in heated channels, Battelle Memorial Institute Report BMI-1517 (May 1961).
10. J. F. MARCHATERRE *et al.*, Natural and forced circulation boiling studies, ANL-5735 (May 1960).
11. H. CHRISTENSEN, Power to void transfer function ANL-6385 (1961).
12. F. W. STAUB *et al.*, Heat transfer and hydraulics; the effects of subcooled voids, NYO-3679-8 (May 1969).
13. L. M. JIJI and J. A. CLARK, Bubble boundary layer and temperature profiles for forced convection boiling in channel flow, *J. Heat Transfer* **86**, 50–58 (1964).
14. N. ZUBER *et al.*, A program of two-phase flow investigation, Eleventh Quarterly Report, GEAP-5067 (Jan. 1966).

15. N. ZUBER *et al.*, A program of two-phase flow investigation, Thirteenth Quarterly Report, GEAP-5203 (July 1966).
16. S. G. BANKOFF, A variable density, single fluid model for two-phase flow with particular reference to steam–water flow, *J. Heat Transfer* **82** 286 (1960).
17. R. D. RICHTMYER and K. MORTON, *Difference Methods for Initial-Value Problems*, 2nd edn. Interscience, New York (1967).
18. C. F. FORREST *et al.*, Axial void distribution in forced convection boiling; a survey of prediction techniques and their efficacy, Submitted for publication in the *J. Heat Transfer* (1970).

APPENDIX I

Closed Form Solution to the Void Propagation Equation

In general the void and enthalpy propagation equations must be solved simultaneously, since the vapour generation function $\langle\Gamma\rangle$ is dependent on both the local void fraction and liquid subcooling, and hence we must resort to numerical techniques. However, in the special case of a thermal equilibrium flow the vapour generation rate is defined explicitly by the energy equation and, for this case the void propagation equation can be solved by the method of characteristics for both inlet flow and heat flux modulation; these solutions have been discussed in some detail by Zuber and Staub.†

The void propagation equation is defined as

$$\frac{\partial\langle\alpha\rangle}{\partial t} + V_\alpha \frac{\partial\langle\alpha\rangle}{\partial z} = \Omega_\alpha \tag{A.1}$$

where

$$V_\alpha = \left[C_0 + \frac{\partial C_0}{\partial\langle\alpha\rangle}\langle\alpha\rangle\right]\langle v\rangle$$

$$\Omega_\alpha = \left[1 - C_0\langle\alpha\rangle\frac{\Delta\rho}{\rho_l}\right]\frac{\langle\Gamma\rangle}{\rho_v}.$$

The left hand side of equation (A.1) is the total derivative of $\langle\alpha\rangle$, hence

$$\frac{d\langle\alpha\rangle}{dt} = \Omega_\alpha \tag{A.2}$$

which defines the void fraction variation of a fluid element as it moves downstream. It follows that velocity of propagation is

$$\frac{dz}{dt} = V_\alpha. \tag{A.3}$$

If Ω_α and V_α are integrable functions, equations (A.2) and (A.3) can be readily solved in closed form.

† N. ZUBER and F. STAUB, The propagation and the wave form of the vapour volumetric concentration in boiling, forced convection systems under oscillatory conditions, *Int. J. Heat Mass Transfer* **9**, 871–895 (1966).

Heat flux modulation

Zuber and Staub have presented the solution to equation (A.1) for a thermal equilibrium flow with C_0 = constant under the following boundary and initial conditions:

(i) heat flux

$$\dot{q}'' = \dot{q}_0''(1 + \varepsilon \sin wt)$$

(ii) constant inlet velocity
(iii) $\langle\alpha\rangle = 0$ at $Z = 0$ for all t.

An approximate closed form solution, for case in which the effect of the oscillations on the propagation velocity is neglected, is presented in form of parametric equations as follows:

$$t^* - t_0^* = \ln(1 + \Gamma_0^* Z^*)/\Gamma_0^* \tag{A.4}$$

$$\alpha^* = 1 - \exp[-\Gamma_0^*(t^* - t_0^*)] \exp\left[\frac{\Gamma_0^*\varepsilon}{\omega^*}(\cos\omega^* t^* - \cos\omega^* t_0^*)\right] \tag{A.5}$$

where

$$t^* = t_0^* \text{ for } z^* = 0 \text{ and } \alpha^* = 0$$
$$\alpha^* = C_0\Delta\rho\langle\alpha\rangle/\rho_f$$
$$t^* = C_0 v_i t/z_h$$
$$\Gamma_0^* = \Delta\rho\, z_h\langle\Gamma\rangle/\rho_f\rho_g v_i$$
$$\omega^* = z_h\omega/C_0 v_i.$$

At a given spatial location, the condition for a maximum or minimum is $\partial\alpha^*/\partial t^*|\, z^* = 0$ and noting that $\partial\alpha^*/\partial t^*|\, z^* = \partial\alpha^*/\partial t_0^*|\, z^*$, equation (A.5) can be differentiated to obtain the following condition for a mximum or minimum

$$\cos(\omega^* t_0^* + \phi/2) = 0 \tag{A.6}$$

where

$$\phi = \frac{\omega^*}{\Gamma_0^*}\ln(1 + \Gamma_0^* z^*).$$

Equation (A.5) is satisfied for

$$\omega^* t_0^* + \phi/2 = \frac{(2n+1)\pi}{2} \quad n = 0, 1, 2, \ldots\ldots$$

and therefore

$$\alpha^*|_{\min}^{\max} = 1 - \frac{\exp\left[-\frac{2\Gamma_0^*\varepsilon}{\omega^*}\sin\phi/2 \sin\frac{(2n+1)\pi}{2}\right]}{1 + \Gamma_0^* z^*}. \tag{A.7}$$

The peak to peak void amplitude, from (A.7), is

$$\Delta\alpha_{pp}^* = \frac{2\left|\sinh\left[\frac{2\Gamma_0^*\varepsilon}{\omega^*}\sin\phi/2\right]\right|}{1 + \Gamma_0^* z^*}. \tag{A.8}$$

We note that $\Delta\alpha^*_{pp} = 0$ for $\phi/2 = n\pi$ and therefore

$$\omega^*|_{\Delta\alpha^*=0} = \frac{2n\pi\Gamma^*_0}{\ln(1+\Gamma^*_0 z^*)}. \tag{A.9}$$

From equation (A.4), the time at which α^* is a maximum or minimum is

$$t^*|_{\alpha^*{}^{\max}_{\min}} = \frac{(2n+1)\pi}{2\omega^*} + \frac{\phi}{2\omega^*}.$$

Noting that the heat flux will have a maximum or minimum value for

$$t^*|_{q''{}^{\max}_{\min}} = \frac{(2n+1)\pi}{2\omega^*}$$

it follows that the phase shift is given by

$$\tau = \frac{\phi}{2\omega^*}$$

and expressed as a phase angle the above equation becomes

$$\Phi = \frac{\omega^*}{2\Gamma^*_0}\ln(1+\Gamma^* z^*). \tag{A.10}$$

APPENDIX II

Finite Difference Solution for the Propagation Equation

A solution is required for the following partial differential equation

$$\frac{\partial\phi}{\partial t} + V\frac{\partial\phi}{\partial Z} = \Omega \tag{A.11}$$

where V and Ω are known functions of t, z and ϕ.

We will make use of the following finite difference relations:

$$\left[\frac{\partial\phi}{\partial t}\right]^{n+\frac{1}{2}}_m \simeq \frac{\phi^{n+1}_m - \phi^n_m}{\Delta t}$$

$$\left[\frac{\partial\phi}{\partial Z}\right]^{n+\frac{1}{2}}_m = \frac{1}{2}\left[\frac{\phi^{n+1}_{m+1} - \phi^{n+1}_{m-1}}{2\Delta Z} + \frac{\phi^n_{m+1} - \phi^n_{m-1}}{2\Delta Z}\right].$$

where n denotes the time increment and m denotes the space increment.

Employing the above relations we obtain the following implicit finite difference analogue of equation (A.11)

$$\frac{\phi^{n+1}_m - \phi^n_m}{\Delta t} = \Omega^n_m - \frac{V^n_m}{4\Delta Z}[\phi^{n+1}_{m+1} - \phi^{n+1}_{m-1} + \phi^n_{m+1} - \phi^n_{m-1}]$$

which may be rearranged to obtain

$$-A^n_m\phi^{n+1}_{m-1} + \phi^{n+1}_m + A^n_m\phi^{n+1}_{m-1} = B^n_m \tag{A.12}$$

where

$$A^n_m = \frac{V^n_m\Delta t}{4\Delta Z}$$

$$B^n_m = \Omega^n_m\Delta t + \phi^n_m - A^n_m(\phi^n_{m+1} - \phi^n_{m-1}).$$

It can be shown that an implicit solution of the form of (A.12) is inherently stable, i.e. numerical disturbances do not grow without bound with increasing time but decay for all space and time step sizes.

Given the following initial conditions,

(i) ϕ^0_m $m = 0, 1, 2, \ldots, M$

(ii) ϕ^n_0 $n = 0, 1, 2, \ldots, N$.

Employing equation (A.12) we can write the following set of M linear equations

$$\begin{aligned}
\phi^{n+1}_1 + A^n_1\phi^{n+1}_2 \qquad\qquad &= B^n_1 - A^n_1\phi^{n+1}_0\\
-A^n_2\phi^{n+1}_1 + \phi^{n+1}_2 + A^n_2\phi^{n+1}_3 &= B^n_2\\
\vdots\qquad\qquad &\quad\vdots\\
-A^n_M\phi^{n+1}_{M-1} + \phi^{n+1}_M + A^n_M\phi^{n+1}_{M+1} &= B^n_M.
\end{aligned}$$

To terminate the calculations at $m = M$ we impose the following constant slope exit condition

$$\left[\frac{\partial\phi}{\partial Z}\right]^n_{M-\frac{1}{2}} = \left[\frac{\partial\phi}{\partial Z}\right]^n_{M+\frac{1}{2}} \qquad n = 0, 1, 2, \ldots, N$$

which becomes in finite difference form

$$\phi_{M+1} = 2\phi_M - \phi_{M-1}.$$

Substitution in the Mth difference equation yields

$$\begin{aligned}
-A^n_M\phi^{n+1}_{M-1} + 1/2(1 + 2A^n_M)\phi^{n+1}_M = 1/2\Omega^n_M\Delta t\\
- A^n_M(\phi^n_M - \phi^n_{M-1}) + 1/2\phi^n_M.
\end{aligned}$$

We now have M equations in M unknowns which can be written in the following matrix form

$$\begin{bmatrix}
1 & A_1 & & & & \\
-A_2 & 1 & A_2 & & & \\
 & -A_3 & 1 & A_3 & & \\
 & & & \ddots & & \\
 & & & -A_{M-1} & 1 & A_{M-1}\\
 & & & & -A_M & \frac{1+2A_M}{2}
\end{bmatrix}^n
\begin{bmatrix}\phi_1\\ \phi_2\\ \phi_3\\ \vdots\\ \phi_{M-1}\\ \phi_M\end{bmatrix}^{n+1}
=
\begin{bmatrix}B'_1\\ B_2\\ B_3\\ \\ B_{M-1}\\ B'_M\end{bmatrix}^n$$

where

$$B'_1 = B_1 - A_1^n \phi_0^{n+1}$$

$$B'_M = 1/2\Omega_M^n \Delta t - A_M^n(\phi_M^n - \phi_{M-1}^n) + 1/2\phi_M^n.$$

Employing the Gaussian elimination technique we arrive at the following solution algorithm for the above set of linear equations

$$\phi_M = E_M/C_M$$

$$\phi_i = (E_i - \phi_{i+1}B_i)/C_i \qquad i = 1, 2, \ldots, M-1$$

where

$$C_1 = 1$$

$$C_i = 1 + \frac{A_{i-1}A_i}{C_{i-1}} \qquad i = 2, 3, \ldots, M-1$$

$$C_M = 1/2(1 + 2A_M) + \frac{A_{M-1}A_M}{C_{M-1}}$$

$$E_1 = B'_1$$

$$E_i = B_i + \frac{E_{i-1}A_i}{C_{i-1}} \qquad i = 2, 3, \ldots, M-1$$

$$E_M = B'_M + \frac{E_{M-1}A_M}{C_{M-1}}.$$

UNE TECHNIQUE GÉNÉRALE POUR ÉVALUER LES DISTRIBUTIONS DE VIDE DANS LA CONVECTION FORCÉE BIPHASIQUE INSTATIONNAIRE

Résumé—On présente une technique analytique pour l'évaluation des distributions instationnaires de vide et d'enthalpie dans la convection forcée d'un écoulement d'eau bouillante. L'analyse est basée sur la forme résultant d'une moyenne dans la section des équations de conservation de masse et d'energie. Des relations auxiliaires basées sur des hypothèses de condition locale sont développées pour décrire: (1) l'effet des profils non uniformes de vide et de vitesse et (2) le taux de vapeur créée. Des estimations de distributions de vide pour un écoulement axial stationnaire sont montrées être en bon accord avec les expériences disponibles, ainsi que l'estimation de l'amplitude d'oscillation de vide et du déphasage du flux thermique modulé.

EINE ALLGEMEINE METHODE ZUR BESTIMMUNG VON DAMPFANTEILEN BEI INSTATIONÄRER, ERZWUNGENER ZWEIPHASENSTRÖMUNG

Zusammenfassung—Es wird eine analytische Methode angegeben zur Bestimmung von instationären Dampf- und Enthalpieverteilungen bei erzwungener Konvektion. Die Berechnung stützt sich auf die über den Querschnitt gemittelte Form der Massen- und der Energieerhaltungsgleichungen. Hilfsbeziehungen für lokale Zustandshypothese wurden entwickelt zur Beschreibung (1) des Einflusses ungleichmässiger Dampfanteil- und Geschwindigkeitsverteilung und (2) der Dampferzeugungsrate. Voraussagen über die achsiale Dampfverteilung vei stetiger Strömung zeigten sich in guter Übereinstimmung mit den verfügbaren Daten, wie auch die Bestimmung der Dampfanteil-Schwankungs-Amplitude und Phasenverschiebung für modulierte Wärmestromwerte.

ОБЩАЯ МЕТОДИКА РАСЧЕТА РАСПРЕДЕЛЕНИЯ ПАРОВОЙ ФАЗЫ ПРИ НЕСТАЦИОНАРНОЙ ВЫНУЖДЕННОЙ КОНВЕКЦИИ В ДВУХФАЗНОЙ ЖИДКОСТИ

Аннотация—Приводится методика аналитического расчета нестационарного распределения объемного паросодержания и энтальпии при кипении воды при вынужденной конвекции. Анализ основан на уравнениях сохранения энергии и массы, осредненых по поперечному сечению. Выведены вспомогательные соотношения на базе гипотезы с локальным условием для описания (1) влияния неоднородных профилей распределения объемного паросодержания и скорости и (2) скорости парообразования. Показано, что результаты расчетов аксиального распределения объемного паросодержания при стационарном течении хорошо согласуются с имеющимися данными, так же как и данные расчетов амплитуды колебаний паросодержания и скорости фазы в случае модулированного теплового потока.